

# A Digital Reverberation Simulator Based On Multi-Port Acoustic Elements\*

Warren L. G. Koontz, SungYoung Kim, Mark J. Indelicato  
College of Applied Science and Technology  
Rochester Institute of Technology  
Rochester, NY USA

**Abstract**—Networks of multi-port acoustic elements can be used to model acoustic systems and process audio signals. In this paper we introduce a simple waveguide network structure designed to add a reverberation effect to an audio signal. The resulting processor is computationally efficient and exhibits an impulse response characteristic of a reverberant space. We include the results of listener comparisons among this and two well-known approaches.

**Keywords**—audio signal processing; artificial reverberation;

## I. INTRODUCTION

As discussed in [1], networks of multi-port acoustic elements can be used for acoustic system modeling, audio signal processing and other applications. In this paper, we concentrate on a particular audio signal processing application: digital reverberation simulators (DRS). DRS began to appear in the early 1960s [2] and several approaches to DRS design appear in [3]. We develop a DRS using a few of the multi-port acoustic elements presented in [1]. The result is a simple example of a distributed waveguide network (DWN) as defined in [4]. It can also be viewed as a more general version of a feedback delay network (FDN) [5].

Artificial reverberation is a popular audio effect that, at least when not overdone, adds a pleasing quality to performed or recorded music or other audio. When you hear music played in a acoustically well-designed concert hall or church, the various sounds are sustained such that the more recent sounds are blended with remnants of previous sounds to give the listener a feeling for the dynamics of the sound in both time and space. The impulsive sound of, say, a starter's pistol, which might sound like a short loud "pop" in an open field, may be heard for several seconds in a "live" hall. The basic reason for this is that in an enclosed space with reflective surfaces, sound travels from the source to the listener over multiple paths and each path can have a unique combination of delay, attenuation and frequency shaping. The delay depends on the length of the path and a path including many reflections will have noticeably more delay than a direct path from the source to the listener. Attenuation and frequency shaping depend on characteristics of the reflecting surfaces and acoustic properties of the atmosphere in the performance space.

The goal of a DRS is to simulate the effect of a reverberant space on audio by means of audio signal processing. Early reverb simulators processed the audio as an analog acoustic signal mechanically using plates or springs. Our focus, however, is on digital audio signal processing algorithms that can be implemented in software to run on a digital audio workstation (DAW) or even a general purpose computer. In particular, we wish to design a digital filter that has an impulse response (IR) similar to that of a reverberant space.

Perhaps the most straightforward approach to DRS design is to measure the impulse response of a reverberant space and use this measured response to process and audio signal via convolution. This approach has been made practical by the development of fast convolution algorithms, such as the overlap-save and overlap-add methods [6]. Moreover, robust measurement techniques, especially the swept-sine method [7], provide excellent replications of the impulse responses of real spaces. Thus a DRS using measured impulse response is one of the competitors in the listener comparison tests presented later on.

Other approaches to DRS design attempt to mimic the impulse response of a reverberant space without explicitly measuring it. For example, one might proceed as follows:

- Determine some basic characteristics of the impulse response of a reverberant space.
- Design a digital filter with an impulse response that has those characteristics.
- Leave some parameters open for the listener to adjust to his or her liking.

The impulse response  $h(n)$  of a reverberant space has the following characteristics:

- $h(n) = 0$  for  $n < 0$  (realizable)
- $h(n)$  generally (but not necessarily consistently) decreases exponentially with increasing  $n$
- The density of non-zero  $h(n)$  increases with increasing  $n$

The second characteristic reflects the fact that the sound energy is eventually absorbed by the space and the exponential nature of the decay was initially described by Sabine [8]. The third characteristic follows from the fact that the first "copies" of the

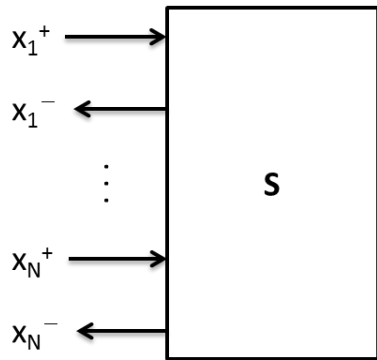


Figure 1 - Multi-Port Acoustic Element

impulse to reach the listener follow a small number of relatively straightforward paths involving only a few reflections. With passing time, however, the impulse copies find more and more ways to reach the listener and their arrival rate increases, ultimately resembling a statistical noise process. These two phases of the response are often referred to as *early reflections* and *late reverberation*, respectively.

The remainder of this paper is organized as follows: Section II reviews the multi-port acoustic elements presented in [1], which are characterized by *scattering matrices*. Section III develops the associated DRS. Section IV presents the impulse response of the DRS and compares it with measured responses and the IR of the well-known Schroeder system [2]. Section V presents the results of listener comparison tests.

## II. MULTI-PORT ACOUSTIC ELEMENTS

Fig. 1 illustrates a general multi-port acoustic element. There are  $N$  ports numbered 1 through  $N$  and each port has an entering (denoted +) and an exiting (denoted -) plane acoustic wave characterized by a complex amplitude. The exiting waves are related to the entering waves by the scattering matrix  $S$  as

$$\mathbf{X}^- = \mathbf{S}\mathbf{X}^+ \quad (1)$$

where  $\mathbf{X}$  is a vector of the wave amplitudes.

Our DRS uses two types of elements: the *multi-port junction*, which is the intersection of  $N$  acoustic waveguides with given cross-section areas and the *waveguide bank*, which is a set of  $N$  parallel acoustic waveguides. The scattering matrix for the a multi-port junction is shown in [1] to be

$$\mathbf{S} = \frac{2}{\sum_{n=1}^N a_n} \begin{bmatrix} a_1 & \cdots & a_N \\ \vdots & \ddots & \vdots \\ a_1 & \cdots & a_N \end{bmatrix} - \mathbf{I} \quad (2)$$

where  $a_n$  is the cross-section area of port  $n$ .

Fig. 2 illustrates the waveguide bank. In this case, the multi-port model is a parallel arrangement of  $N$  two-port models, each with an  $x$  side and a  $y$  side. For each waveguide, we have

$$\begin{bmatrix} x_n^- \\ y_n^- \end{bmatrix} = \begin{bmatrix} 0 & e^{-\gamma L_n} \\ e^{-\gamma L_n} & 0 \end{bmatrix} \begin{bmatrix} x_n^+ \\ y_n^+ \end{bmatrix} \quad (3)$$

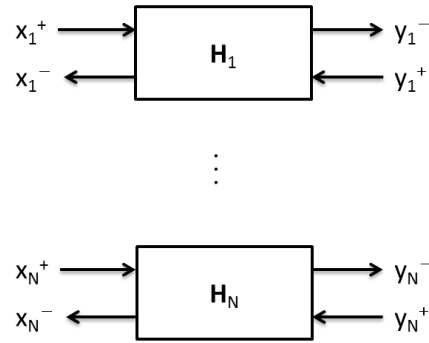


Figure 2 - Waveguide Bank

We can express this more compactly as

$$\begin{aligned} \mathbf{X}^- &= \mathbf{H}\mathbf{Y}^+ \\ \mathbf{Y}^- &= \mathbf{H}\mathbf{X}^+ \end{aligned} \quad (4)$$

where

$$\mathbf{H} = \begin{bmatrix} h_1 & 0 & \cdots & 0 \\ 0 & h_2 & \cdots & 0 \\ \vdots & \vdots & \ddots & \vdots \\ 0 & 0 & \cdots & h_N \end{bmatrix} \quad (5)$$

and

$$h_n = e^{-\gamma L_n} \quad (6)$$

$L_n$  is the length of waveguide  $n$  and  $\gamma$  is the complex propagation factor.

The  $h_n$  can be expressed in terms of the real ( $\alpha$ ) and imaginary ( $\beta$ ) parts of the propagation factor, both of which depend on the frequency  $\omega$  (in radians/second).

$$\begin{aligned} h_n(\omega) &= e^{-(\alpha+j\beta)L_n} \\ &= e^{-\alpha(\omega)L_n} e^{-j\omega L_n/v} \\ &= e^{-T_n/\tau(\omega)} e^{-j\omega T_n} \end{aligned} \quad (7)$$

where  $v$  is the velocity of sound. Thus each waveguide in the bank introduces a propagation delay  $T_n$  and a frequency-dependent attenuation that increases with  $T_n$  and is characterized by a frequency-dependent decay time constant  $\tau(\omega)$ .

The attenuation factor  $e^{-T_n/\tau(\omega)}$  can also be expressed in terms of the *reverberation time*  $T_{60}$ , the time required for the sound to decay by 60 dB.

$$e^{-T_n/\tau(\omega)} = 10^{3T_n/T_{60}(\omega)} \quad (8)$$

The reverberation time and the decay time constant are related as

$$T_{60}(\omega) = 3 \log_{10} \tau(\omega) \quad (9)$$

In a discrete time system, which is our main interest here, the waveguide bank equations become

$$\begin{aligned} \mathbf{X}^-(z) &= \mathbf{H}(z)\mathbf{Y}^+(z) \\ \mathbf{Y}^-(z) &= \mathbf{H}(z)\mathbf{X}^+(z) \end{aligned} \quad (10)$$

where  $\mathbf{H}(z)$  is a diagonal matrix with elements  $h_n(z)$  given by

$$h_n(z) = f_n(z)z^{-M_n} \quad (11)$$

The factor  $f_n(z)$  accounts for the frequency dependent attenuation and  $M_n$  is the propagation delay in samples ( $M_n = f_s T_n$  rounded to the nearest integer, where  $f_s$  is the sampling rate). We will model the attenuation as a first order filter of the form

$$f_n(z) = \frac{g_n}{1 - d_n z^{-1}} \quad (12)$$

The matrix  $\mathbf{H}(z)$  is therefore given by

$$\mathbf{H}(z) = \begin{bmatrix} \frac{g_1}{1 - d_1 z^{-1}} & 0 & \cdots & 0 \\ 0 & \frac{g_2}{1 - d_2 z^{-1}} & \cdots & 0 \\ \vdots & \vdots & \ddots & \vdots \\ 0 & 0 & \cdots & \frac{g_N}{1 - d_N z^{-1}} \end{bmatrix} \quad (13)$$

When  $\mathbf{H}(z)$  is defined by (13), the discrete time version of the waveguide bank equations (10) becomes a set of difference equations, i.e., for  $n = 1, 2, \dots, N$

$$\begin{aligned} x_n(k)^- &= d_n x_n(k-1)^- + g_n y_n(k - M_n)^+ \\ y_n(k)^- &= d_n y_n(k-1)^- + g_n x_n(k - M_n)^+ \end{aligned} \quad (14)$$

These equations can be implemented quite efficiently using buffers.

We can determine suitable values for the  $g_n$  and  $d_n$  in terms of the reverberation time  $T_{60}$ . The magnitude of the attenuation varies between  $g_n/(1 - d_n)$  at frequency  $f = 0$  and  $g_n/(1 + d_n)$  at the Nyquist frequency  $f = f_s/2$ . Given the values of  $T_{60}$  at these two frequencies, we can determine  $g_n$  and  $d_n$  from

$$\begin{aligned} \frac{g_n}{1 - d_n} &= 10^{-3T_n/T_{60}^{LF}} \\ \frac{g_n}{1 + d_n} &= 10^{-3T_n/T_{60}^{HF}} \end{aligned} \quad (15)$$

where  $T_{60}^{LF}$  is the reverberation time at frequency  $f = 0$  and  $T_{60}^{HF}$  is the reverberation time at the Nyquist frequency.

### III. STRUCTURE OF THE DRS

Fig. 3 illustrates the reverberation network, which consists of two identical multiport junctions interconnected by a waveguide bank. Each junction has  $N + 1$  ports: an external port with input/output denoted  $u_1/y_2$  (left) and  $u_2/y_1$  (right) and  $N$  internal ports connecting to the waveguide bank with (vector) input/output denoted  $X_1$  (left) and  $X_2$  (right). The cross-section area of each internal port is  $a$  and the cross-section area of each external port is  $Na$ .

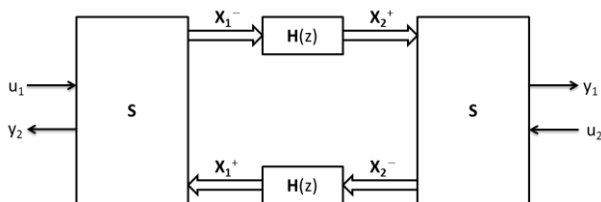


Figure 3 - DRS Structure

This is a simple DWN with two nodes (the multi-port junctions) and  $N + 2$  two-way branches (the  $N$  waveguides plus the two external ports). If we order the ports as the internal ports followed by the external port, the scattering matrix becomes

$$\mathbf{S} = \frac{1}{Na} \begin{bmatrix} a & \cdots & a & Na \\ \vdots & \ddots & \vdots & \vdots \\ a & \cdots & a & Na \end{bmatrix} - \mathbf{I} \quad (16)$$

$$= \begin{bmatrix} \mathbf{A} & \mathbf{B} \\ \mathbf{C} & \mathbf{0} \end{bmatrix}$$

where

$$\mathbf{A} = \frac{1}{N} \mathbf{O} - \mathbf{I} \quad (17)$$

$$\mathbf{B} = [1 \quad \cdots \quad 1]^T$$

$$\mathbf{C} = [1 \quad \cdots \quad 1]$$

and  $\mathbf{O}$  is an  $N \times N$  matrix of ones. Thus the port variables are related by the junctions as

$$X_1^- = \mathbf{A}X_1^+ + \mathbf{B}u_1$$

$$X_2^- = \mathbf{A}X_2^+ + \mathbf{B}u_2$$

$$y_1 = \mathbf{C}X_2^+$$

$$y_2 = \mathbf{C}X_1^+$$

Note that setting the cross-section area of the external ports to  $Na$  results in an acoustic impedance match between the external ports and the combination of the internal ports so that there is no *direct* reflection of the external inputs. If this were not the case, the 0 in  $\mathbf{S}$  would be replaced by a scalar value  $D$ . Note also that because of the simple structures of  $\mathbf{A}$ ,  $\mathbf{B}$ , and  $\mathbf{C}$ , the calculation of (18) is  $O(N)$  rather than  $O(N^2)$ .

The interior input/output vectors are related by the waveguide bank equations as

$$X_1^+(z) = \mathbf{H}(z)X_2^-(z) \quad (19)$$

$$X_2^+(z) = \mathbf{H}(z)X_1^-(z)$$

Equations (18) and (19) can be written in a more compact matrix form as

$$X^- = \mathbf{A}^*X^+ + \mathbf{B}^*U$$

$$Y = \mathbf{C}^*X^+$$

and

$$X^+(z) = \mathbf{H}^*(z)X^-(z) \quad (21)$$

where

$$\mathbf{A}^* = \begin{bmatrix} \mathbf{A} & \mathbf{0} \\ \mathbf{0} & \mathbf{A} \end{bmatrix}$$

$$\mathbf{B}^* = \begin{bmatrix} \mathbf{B} & \mathbf{0} \\ \mathbf{0} & \mathbf{B} \end{bmatrix} \quad (22)$$

$$\mathbf{C}^* = \begin{bmatrix} \mathbf{0} & \mathbf{C} \\ \mathbf{C} & \mathbf{0} \end{bmatrix}$$

and

$$\mathbf{H}^*(z) = \begin{bmatrix} \mathbf{0} & \mathbf{H}(z) \\ \mathbf{H}(z) & \mathbf{0} \end{bmatrix} \quad (23)$$

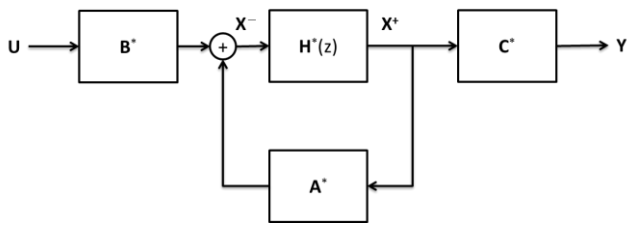


Figure 4 - Feedback Delay Network Model of the DRS

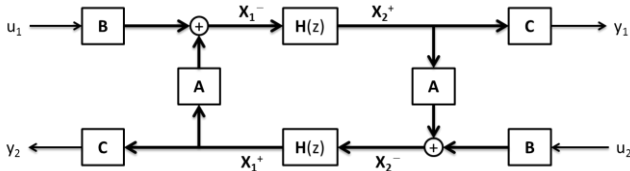


Figure 5 - Signal Flow Graph Model

In this compact form our DRS becomes a feedback delay network with multiple inputs and outputs as shown in Fig. 4.

Equations (18) and (19) can be displayed as a signal flow graph as shown in Fig. 5. The signal flow graph model suggests that, viewed from a sufficient distance, our DRS is a two-port system. In fact the external input/output ports are related by a  $2 \times 2$  scattering matrix with elements

$$\begin{bmatrix} y_2 \\ y_1 \end{bmatrix} = \begin{bmatrix} S_{11} & S_{12} \\ S_{21} & S_{22} \end{bmatrix} \begin{bmatrix} u_1 \\ u_2 \end{bmatrix} \quad (24)$$

where

$$\begin{aligned} S_{11} &= S_{22} = \mathbf{CH}(z)\{\mathbf{I} - [\mathbf{AH}(z)]^2\}^{-1}\mathbf{AH}(z)\mathbf{B} \\ S_{12} &= S_{21} = \mathbf{CH}(z)\{\mathbf{I} - [\mathbf{AH}(z)]^2\}^{-1}\mathbf{B} \end{aligned} \quad (25)$$

It can be shown that if all of the waveguides in the bank are identical, i.e.,  $\mathbf{H}(z) = h(z)\mathbf{I}$ , then

$$\begin{aligned} S_{11} &= S_{22} = 0 \\ S_{12} &= S_{21} = h(z) \end{aligned} \quad (26)$$

a simple but not very useful result. When  $\mathbf{H}(z)$  is given by (13) with a suitable mix of the  $M_n$ , however, the system can be used to create artificial reverberation. This can be explained qualitatively with the help of Fig. 3. Consider an audio impulse signal  $u_1$  entering the system on the left-hand side. This signal is split equally by the junction into  $N$  signals that enter the waveguide bank. These signals reach the right-hand junction at different times and with different amplitudes (and shapes, because of dispersion) due to the varying lengths of the waveguides. Each signal is partially transmitted as part of  $y_1$  and partially reflected back into the waveguide bank, incurring another split (this one not quite even). The reflected signals return to the left-hand junction where they are partially transmitted as part of  $y_2$  and partially reflected back toward the right-hand junction. With the passage of time, the number of signals keeps increasing by  $N$  while the signals lose amplitude due to the splitting as well as attenuation. Thus the outputs  $y_1$  and  $y_2$  are streams of

impulses with generally decreasing amplitude and increasing density, as desired.

Let us now address how to obtain our suitable mix of the  $M_n$ . If all of the  $M_n$  are equal, then all of the  $h_n(z)$  will be equal and we get the trivial result as stated earlier. The situation is not much better if all of the  $M_n$  are multiples of some fundamental sample delay. This is because the sample delay of a given path from input to output is of the form

$$\Delta = \sum_{n \in P} M_n \quad (27)$$

where  $P$  is a sequence of waveguide indices for a path through the system. Thus all delays will be some multiple of the fundamental delay and the output density will be limited. It is generally recommended that the delays used in artificial reverberation algorithms be *mutually prime*, a condition that is certainly satisfied if all the delays are prime numbers. Our approach is to choose a maximum delay  $M_{max}$  and a minimum delay  $M_{min}$  and generate a set of  $N$  delays as follows:

$$M_n = \text{lowprime}(\alpha^{n-1}M_{max}) \quad (28)$$

where  $\text{lowprime}(x)$  is the largest prime number less than or equal to  $x$  and

$$\alpha = \left(\frac{M_{min}}{M_{max}}\right)^{\frac{1}{N-1}} \quad (29)$$

This will produce a roughly exponential sequence of prime delays over the specified range of delays.

In summary, this DRS can be viewed as a simple waveguide network, a feedback delay network, a two-port acoustic element or just another IIR filter. Qualitative arguments indicate that it can add a reverberation effect to an audio signal. In the following sections we will investigate this further by first examining the impulse response of this DRS and comparing it with real and other artificial responses and in Section IV comparing listener evaluations.

#### IV. IMPULSE RESPONSE ANALYSIS AND COMPARISON

##### A. Measured Impulse Response

We begin with IR recorded at the Great Hall, a multi-purpose 800 seat facility at the Mile End campus of Queen Mary, University of London in 2008 [9]. The recordings were made using the sine sweep method [7] using a single source location and a rectangular array of 144 recording locations. Fig. 6 shows two of the recorded impulse responses. The full database shows considerable variation of the IR with the recording location and these two examples are far from exhaustive, even for a single hall. All they provide here is a minimum basis for comparison. All of the IR, however, display early strong responses followed by, and sometimes concurrently with, a decaying noise-like response.

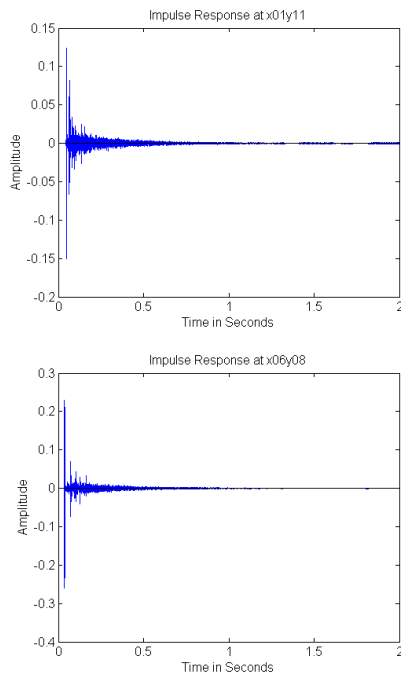


Figure 6 - Impulse Responses Measured at the Great Hall, University of London

B. Impulse Response of Proposed DRS

The IR of the proposed DRS is determined by simply executing the DRS with a discrete impulse  $\delta(n)$  as the input. Table 1 lists a set of parameters for a typical implementation of the proposed DRS. The resulting delay values are listed in Table 2. Fig. 7 shows the right and left channel responses ( $y_1$  and  $y_2$ ) to a right channel ( $u_1$ ) impulse (no input to left channel) for this instance of the DRS. Both responses display an early reflections and a late reverberation phase and the echo density appears to increase as the response dies out. Fig. 8 provides a closer look at the early reflections phase and the beginning of the late reverberation phase.

Table 1 - DRS Control Parameters

$N$	8
$M_{min}$	500
$M_{max}$	5000
$T_{60}^{LF}$	1.0 seconds
$T_{60}^{HF}$	0.5 seconds

Table 2 - DRS Waveguide Sample Delays

WG Index	Delay	WG Index	Delay
1	4999	5	1327
2	3593	6	953
3	2579	7	691
4	1861	8	499

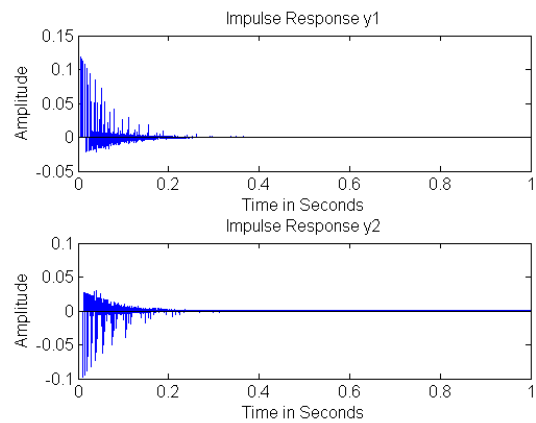


Figure 7 - Impulse Response of Proposed DRS

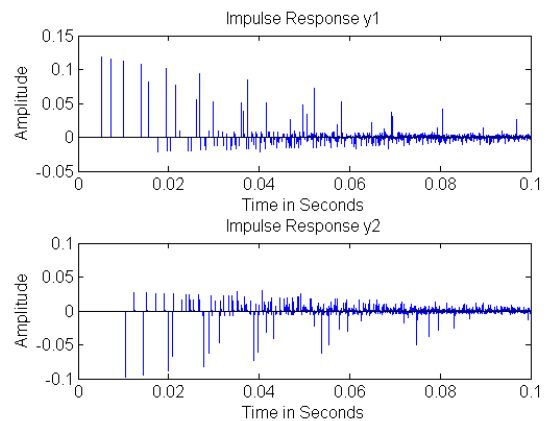


Figure 8 - Early Reflection Phase of DRS Impulse Response

The proposed DRS exhibits the desired properties of a DRS IR listed in Section I, i.e., early and late phases, exponential decay and increasing density. The IR is somewhat more orderly than the real, measured IR, probably due to the simple structure of the underlying network. A real hall is a complex environment that introduces nonlinearities and time-variance not captured in such a simple model.

C. Impulse Response of Schroeder DRS

Schroeder and Logan [2] developed a DRS using a combination of comb filters and all-pass filters. The impulse response of a single comb or all-pass filter is a sequence of impulses with exponentially decreasing amplitudes, like a sequence of echoes. A sufficiently ingenious combination of these filters, however, has an impulse response with the characteristics of a DRS. In particular, a popular system known as *Freeverb*, developed by "Jezar at Dreampoint", uses a parallel combination of eight low-pass comb filters driving a cascade of four all-pass filters, as nicely explained in [3].

A low-pass comb filter is governed by three parameters: a feedback parameter, a damping parameter and a sample delay. An all-pass filter is governed by a feedback parameter and a sample delay. In Freeverb all of the comb filters have the same feedback and damping values and all of the all-pass

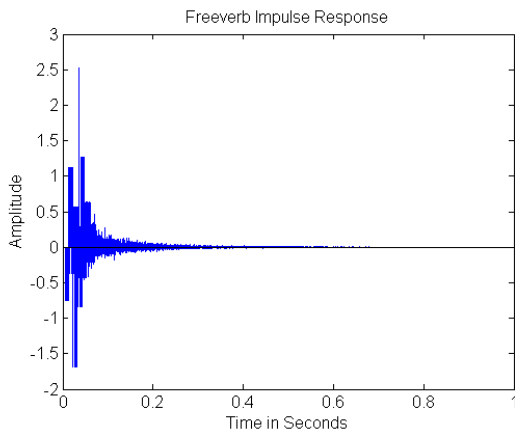


Figure 9 - Freeverb Impulse Response

filters have the same feedback value. Most implementations allow the user to vary one or more of these values. The real contribution of Jezar, however, is the selection of the delay values, which are fixed. It appears that Jezar, and perhaps others, chose these values based on listening to the results of applying Freeverb to audio recordings with a standard sampling rate of 44100 samples/second. Freeverb is implemented for two channel audio using two instances of the system. The delays for the two systems differ by a constant 23 sample delay known as the "stereo separation", which is applied to all of the filters.

Fig. 9 shows the impulse response of a single-channel MATLAB version of Freeverb using Jezar's recommendations for all parameter values (see, e.g., [3]). The early part of the impulse response has a somewhat regular structure while the latter part appears to be decaying white noise. The initial phase of the Freeverb impulse response does not appear to display exponential decay. In fact, the magnitude of the Freeverb impulse response grows initially. However, this supposed shortcoming has not prevented Freeverb from being widely accepted - for example, it is the current default DRS for the Audacity system [10]. We include Freeverb in the listener comparison tests in Section V.

## V. SUBJECTIVE EVALUATION

### A. Stimuli Preparation

The authors conducted a listening test comparing the proposed method with two conventional methods (Freeverb and Altiverb, a convolution-based DRS from Audio Ease). Two sound sources, Drums and Solo Trumpet, were chosen for this experiment, which represented a transient and a legato character of music respectively. First, we configured the proposed method so that it could produce reverberation with convincing realism and satisfactory quality. After several trials, the authors set the parameters of proposed method as follows:  $N = 16$ ,  $T_{60}^{LF} = 2.5$  seconds and  $T_{60}^{HF} = 2.0$  seconds. Next, the other two DRS were configured to reproduce similar acoustic characteristics to the proposed DRS. We selected the

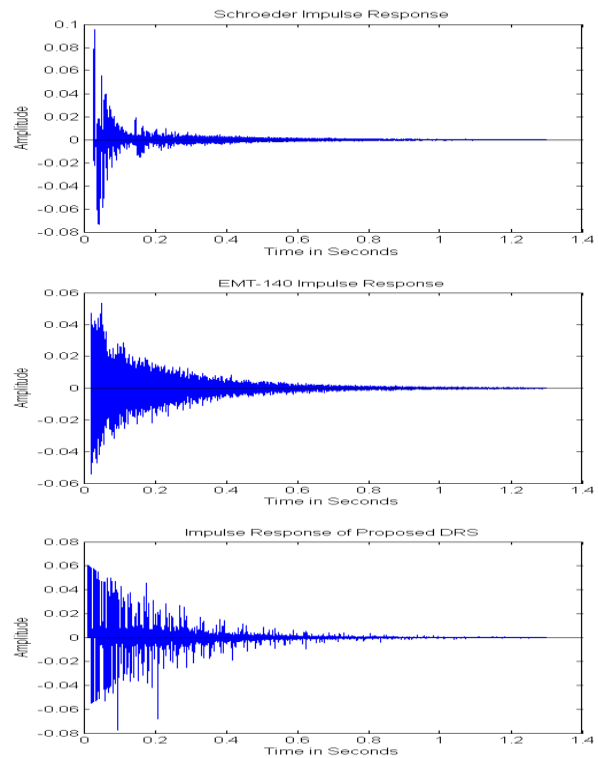


Figure 10 - Impulse Responses of DRS Used in Listener Evaluation

Freeverb "PLATE" algorithm and adjusted the associated parameters to be as consistent as possible with the proposed DRS. We selected the EMT-140 (a plate reverberator) IR for Altiverb and adjusted the parameters for consistency with the other two DRS. Finally, the overall loudness of three rendered IRs were matched so that the listeners would not decide their preferred reverberation based on loudness. Fig. 10 shows the IR for each of the DRS.

### B. Listeners and Peripherals

A total of 25 audio engineering students participated in the experiment. They had previously participated in similar critical listening experiments. Each subject listened to the output of each DRS for the two sound sources. The subjects then ranked the three outputs for each sound source based on his or her personal judgment. The direct question given to the subjects was as follows: "Which DRS do you want to use for your mixing project?" Each subject listened to the outputs using an AVID M-BOX2 audio interface and an AKG K-550 headphone.

### C. Results

Figure 11 shows the Kruskal-Wallis test (equivalent to ANOVA-test for non-parametric data) results of the collected rank data. C1 and C2 indicate the two existing DRS and MR indicates the proposed DRS. The results show that the column effect (DRS type) significantly differentiated the medians of collected rank of DRUM ( $p = 0.0261$ ) as well as TRUMPET ( $p = 0.001$ ), which indicates that the subjects were able to discriminate the three DRS based on their preferences.

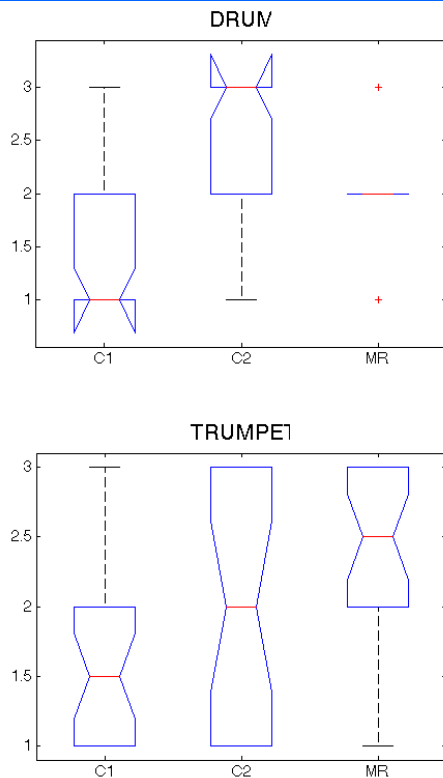


Figure 11 - Kruskal-Wallis Test Results

A subsequent Wilcoxon rank sum test for equal medians revealed that the median of listeners' preferential rank data for C2 is significantly different from C1 ( $p = 0.0126$ ) for DRUM, but not significantly different from MR ( $p = 0.1197$ ). This indicates that listeners' had no greater preference for MR than for C1 or C2 (while C2 was much favored to C1). In contrast, the preference median of MR for TRUMPET is significantly different from C1 ( $p = 0.0011$ ) yet not different from C2 ( $p = 0,0748$ ). As for TRUMPET, listeners preferred MR, at the least, to C1.

The results show that the proposed DRS is comparable and sometimes preferable to existing DRS.

## VI. CONCLUSIONS

Multi-port acoustic elements are useful building blocks for creating audio signal processing applications. In this paper we have developed and analyzed a digital reverberation simulator constructed

from two basic multi-port elements: the multi-port junction and the waveguide bank. The structure is simple and the computational requirements are modest. The proposed DRS has been implemented as a MATLAB script and a C++ plug-in and the latter has been tested successfully in a real-time system. On the basis of IR plots and listener evaluation, the proposed DRS is comparable to Schroeder and convolution-based DRS and has fared well under the scrutiny of experienced listeners.

## REFERENCES

- [1] W. L. G. Koontz, "Multi-Port Acoustic Models with Applications in Audio Signal Processing," *JAES*, 2013.
- [2] M. R. Schroeder and B. Logan, "'Colorless' artificial reverberation," *IRE Transactions on Audio*, Vols. AU-9, no. 6, pp. 209-214, 1961.
- [3] J. O. Smith, *Physical Audio Signal Processing*, Online Book, 2010.
- [4] J. O. Smith, "A New Approach to Digital Reverberation Using Closed Waveguide Networks," in *International Computer Music Conference*, Burnaby, B.C., Canada, 1985.
- [5] J.-M. Jot and A. Chaigne, "Digital Delay Networks for Designing Artificial Reverberators," in *Audio Engineering Society Convention 90*, 1991.
- [6] V. Madisetti, *The Digital Signal Processing Handbook*, Taylor & Francis, 1997.
- [7] A. Farina, "Simultaneous Measurement of Impulse Response and Distortion With a Swept-Sine Technique," in *108th AES Convention*, 2000.
- [8] W. Sabine, *Collected Papers on Acoustics*, Harvard University Press, 1923.
- [9] R. Stewart and M. Sandler, "Database of omnidirectional and B-format room impulse responses," in *2010 IEEE International Conference on Acoustics Speech and Signal Processing*, 2010.
- [10] D. Mazzoni and R. Dannenberg, "A Fast Data Structure for Disk-Based Audio Editing," *Computer Music Journal*, vol. 26, no. 2, 2002.